


Cite this: *RSC Adv.*, 2018, 8, 17677

# Deactivation by HCl of CeO<sub>2</sub>–MoO<sub>3</sub>/TiO<sub>2</sub> catalyst for selective catalytic reduction of NO with NH<sub>3</sub>

Ye Jiang,<sup>a</sup> Mingyuan Lu,<sup>a</sup> Shaojun Liu,<sup>b</sup> Changzhong Bao,<sup>a</sup> Guitao Liang,<sup>a</sup> Chengzhen Lai,<sup>a</sup> Weiyun Shi<sup>a</sup> and Shiyuan Ma<sup>a</sup>

The effect of HCl on a CeO<sub>2</sub>–MoO<sub>3</sub>/TiO<sub>2</sub> catalyst for the selective catalytic reduction of NO with NH<sub>3</sub> was investigated with BET, XRD, NH<sub>3</sub>-TPD, H<sub>2</sub>-TPR, XPS and catalytic activity measurements. The results showed that HCl had an inhibiting effect on the activity of the CeO<sub>2</sub>–MoO<sub>3</sub>/TiO<sub>2</sub> catalyst. The deactivation by HCl of the CeO<sub>2</sub>–MoO<sub>3</sub>/TiO<sub>2</sub> catalyst could be attributed to pore blockage, weakened interaction among ceria, molybdenum and titania, reduction in surface acidity and degradation of redox ability. The Ce<sup>3+</sup>/Ce<sup>4+</sup> redox cycle was damaged because unreactive Ce<sup>3+</sup> in the form of CeCl<sub>3</sub> lost the ability to be converted to active Ce<sup>4+</sup> in the SCR reaction. In addition, a decrease in the amount of chemisorbed oxygen and the concentrations of surface Ce and Mo was also responsible for the deactivation by HCl of the CeO<sub>2</sub>–MoO<sub>3</sub>/TiO<sub>2</sub> catalyst.

Received 10th January 2018  
Accepted 23rd April 2018

DOI: 10.1039/c8ra00280k

rsc.li/rsc-advances

## 1. Introduction

The selective catalytic reduction (SCR) of NO<sub>x</sub> with NH<sub>3</sub> is an efficient technology for the removal of NO<sub>x</sub> in flue gas from stationary sources.<sup>1</sup> V<sub>2</sub>O<sub>5</sub>–WO<sub>3</sub>(MoO<sub>3</sub>)/TiO<sub>2</sub> catalysts have been widely used in the last few decades.<sup>2,3</sup> In recent years, great attention has been paid to develop environment-friendly vanadium-free catalysts for SCR applications mainly owing to the toxicity of vanadium.<sup>4,5</sup> Cerium-based catalysts are regarded as promising candidates due to the high oxygen storage capacity and excellent redox properties of CeO<sub>2</sub>.<sup>4,6,7</sup> Many researchers have developed numerous cerium-based metal oxide catalysts, which possessed good SCR activity, such as MoO<sub>3</sub>/CeO<sub>2</sub>–ZrO<sub>2</sub>,<sup>8</sup> Cu–Ce–Ti oxide,<sup>6,9</sup> Mn–Ce–Ti oxide,<sup>10</sup> *etc.* Our group prepared a CeO<sub>2</sub>–MoO<sub>3</sub>/TiO<sub>2</sub> catalyst using a single step sol-gel method, which exhibited high SCR activity and resistance to 10% H<sub>2</sub>O and 1000 ppm SO<sub>2</sub>.<sup>11</sup> However, from the point of view of industrial applications, further studies are still required to clarify their adaptability to other components in flue gas from stationary sources, such as alkali (earth) metals, heavy metals, HCl, *etc.*

It is well known that HCl is widely present in the flue gas from coal-fired boilers and municipal solid waste (MSW) incinerators. The effect of HCl on SCR catalyst has been investigated by several researchers. Chen *et al.*<sup>12</sup> attributed the deactivation by HCl of V<sub>2</sub>O<sub>5</sub>/TiO<sub>2</sub> catalyst to the formation of volatile vanadium chlorides and NH<sub>4</sub>Cl. Lisi *et al.*<sup>13</sup> reported

that HCl suppressed the SCR activity of commercial V<sub>2</sub>O<sub>5</sub>–WO<sub>3</sub>/TiO<sub>2</sub> catalyst due to the formation of new acid sites showing a lower activity compared to the original one. Yang *et al.*<sup>14</sup> proposed that Cl could inhibit the adsorption of NH<sub>3</sub> and NO<sub>x</sub> species, thereby leading to the deactivation of Ce/TiO<sub>2</sub>. On the contrary, Hou *et al.*<sup>15</sup> found that HCl had a positive effect on the catalytic activity of V<sub>2</sub>O<sub>5</sub>/AC catalyst at 150 °C. As for the effect of HCl on CeO<sub>2</sub>–MoO<sub>3</sub>/TiO<sub>2</sub> catalyst for the SCR of NO with NH<sub>3</sub>, there were few reports to our knowledge till now.

In this work, the effect of HCl on CeO<sub>2</sub>–MoO<sub>3</sub>/TiO<sub>2</sub> catalyst was investigated for the SCR of NO with NH<sub>3</sub>. A series of characterizations, including BET, XRD, XPS, NH<sub>3</sub>-TPD and H<sub>2</sub>-TPR, were performed to provide an insight into the substantial change in CeO<sub>2</sub>–MoO<sub>3</sub>/TiO<sub>2</sub> catalyst caused by HCl.

## 2. Experimental

### 2.1. Catalyst preparation

The CeO<sub>2</sub>–MoO<sub>3</sub>/TiO<sub>2</sub> catalyst was prepared by a single step sol-gel method as reported in our previous study.<sup>11</sup> The mass ratio of CeO<sub>2</sub> : MoO<sub>3</sub> : TiO<sub>2</sub> was 20 : 10 : 100. All chemicals used in the catalyst preparation were purchased from Sino-pharm Chemical Reagent Corp. (Shanghai, China). Except that titanium butoxide (TBOT) was chemically pure, the other reagents were of analytical grade. TBOT, anhydrous ethanol, deionized water, 65–68 wt% nitric acid, cerium nitrate hexahydrate (Ce(NO<sub>3</sub>)<sub>3</sub>·6H<sub>2</sub>O) and ammonium molybdate tetrahydrate ((NH<sub>4</sub>)<sub>6</sub>Mo<sub>7</sub>O<sub>24</sub>·4H<sub>2</sub>O) were mixed at a molar ratio of 1 : 35 : 19 : 2 : 0.1 : 0.1. After continuously stirred for 3 h at room temperature, the solution was kept at 80 °C for 24 h to form xerogel. The obtained xerogel were milled and sieved out,

<sup>a</sup>College of Pipeline and Civil Engineering, China University of Petroleum, 66 Changjiang West Road, Qingdao 266580, P. R. China. E-mail: jiangye@upc.edu.cn; Fax: +86-532-86981882; Tel: +86-532-86981767

<sup>b</sup>State Key Laboratory of Clean Energy Utilization, Zhejiang University, 32 Zheda Road, Hangzhou 310027, China



followed by calcination at 500 °C for 5 h in static air. The catalyst was denoted as CMT.

The HCl-loaded CeO<sub>2</sub>-MoO<sub>3</sub>/TiO<sub>2</sub> catalysts were prepared by impregnation *via* incipient wetness with appropriate hydrochloric acid solution on CMT. The mixture was aged for 24 h and dried at 80 °C for 12 h. The HCl-loaded CeO<sub>2</sub>-MoO<sub>3</sub>/TiO<sub>2</sub> catalysts were denoted as CMT<sub>x</sub>, where *x* represented the molar ratio of Cl and Ce.

## 2.2. Catalyst characterization

BET surface area, total pore volume and average pore diameter were measured by N<sub>2</sub> adsorption and desorption at −196 °C with ASAP2020-M (Micromeritics Instrument Corp.). Prior to the measurement, the sample was degassed in vacuum at 300 °C for 4 h.

X-ray diffraction (XRD) measurement was carried out with on a X'Pert PRO diffractometer (Panalytical Corp.) with Cu K $\alpha$  radiation at 40 kV and 40 mA.

X-ray photoelectron spectroscopy (XPS) data were obtained with a Thermo ESCALAB 250 spectrometer using monochromated Al K $\alpha$  X-rays (*h* $\nu$  = 1486.6 eV) as a radiation source at 150 W. Sample charging effects were eliminated by correcting the observed spectra with the C 1s binding energy (BE) value of 284.6 eV.

Temperature programmed desorption of NH<sub>3</sub> (NH<sub>3</sub>-TPD) and temperature programmed reduction of H<sub>2</sub> (H<sub>2</sub>-TPR) were performed on a FINESORB-3010 chemisorption analyzer (FINETEC Instruments Corp.) with 0.1 g of the catalysts with a thermal conductivity detector (TCD). For NH<sub>3</sub>-TPD, the sample was pretreated at 500 °C in He for 1 h. After cooled down, it was exposed in a 0.5% NH<sub>3</sub>/He (30 mL min<sup>−1</sup>) gas flow for 1 h, followed by flushing with He for 1 h. Finally, the sample was heated up to 700 °C with the rate of 10 °C min<sup>−1</sup> in He. H<sub>2</sub>-TPR were carried out in the flow of H<sub>2</sub> (10%) in Ar (30 mL min<sup>−1</sup>)

from room temperature to 800 °C with the heating rate of 10 °C min<sup>−1</sup>.

## 2.3. SCR activity test

The activity measurements were carried out in a fixed-bed quartz reactor (i.d. = 8 mm) using 0.23 g catalyst with 60–100 mesh at atmospheric pressure in the temperature range of 150–500 °C. The feed gas contained 1000 ppm NO, 1000 ppm NH<sub>3</sub>, 3 vol% O<sub>2</sub>, 10% H<sub>2</sub>O (when used), 500 ppm SO<sub>2</sub> (when used) and N<sub>2</sub> as balance gas. The total flow rate was 500 mL min<sup>−1</sup>, corresponding to a gas hourly space velocity (GHSV) of 150 000 h<sup>−1</sup>. The concentrations of NO, SO<sub>2</sub> and O<sub>2</sub> were continuously monitored by a gas analyzer (350 Pro, Testo). The concentrations of NO<sub>2</sub> and N<sub>2</sub>O were recorded by a FT-IR gas analyzer (DX-4000, Gasmet). The NO conversion and N<sub>2</sub> selectivity of catalysts were calculated by:<sup>16</sup>

$$\text{NO conversion(\%)} = \frac{[\text{NO}]_{\text{in}} - [\text{NO}]_{\text{out}}}{[\text{NO}]_{\text{in}}} \times 100 \quad (1)$$

$$\text{N}_2 \text{ selectivity(\%)} = \left( 1 - \frac{[\text{NO}_2]_{\text{out}} + 2[\text{N}_2\text{O}]_{\text{out}}}{[\text{NO}]_{\text{in}} - [\text{NO}]_{\text{out}}} \right) \times 100 \quad (2)$$

## 3. Results and discussion

### 3.1. NH<sub>3</sub>-SCR performance

Fig. 1 shows the NH<sub>3</sub>-SCR performance of the fresh and HCl-loaded CMT. It could be seen from Fig. 1(a) that the catalytic activity of CMT declined and its active temperature window was shortened with increasing HCl loadings in the temperature range of 150–500 °C. Furthermore, it seemed that the inhibiting effect of HCl on the SCR activity of CMT was more obvious below 300 °C. As for the N<sub>2</sub> selectivity, there was hardly a difference among the three samples at temperatures from

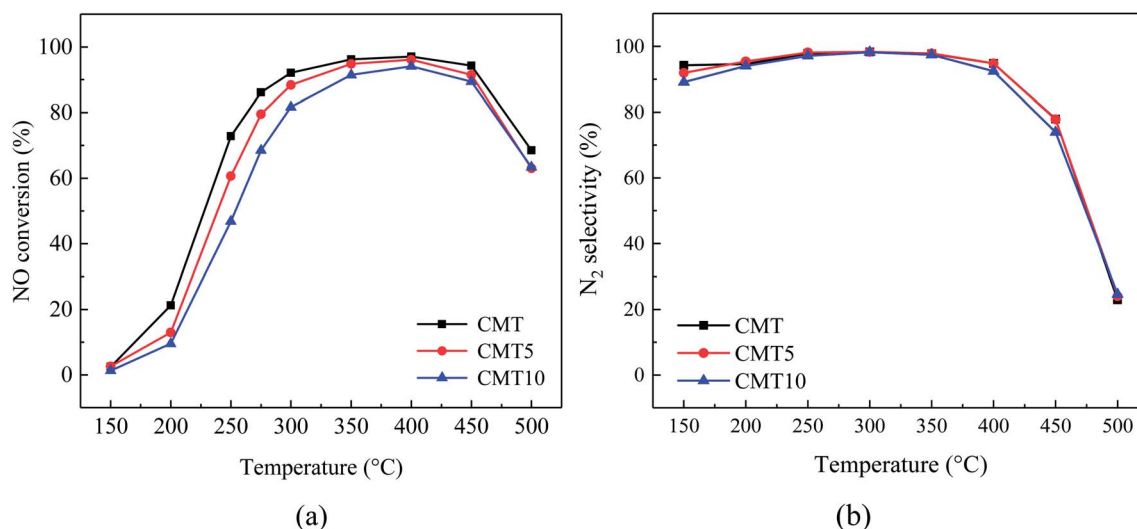


Fig. 1 SCR activity (a) and N<sub>2</sub> selectivity (b) of different samples as a function of reaction temperature. Reaction conditions: [NO] = [NH<sub>3</sub>] = 1000 ppm, [O<sub>2</sub>] = 3%, balance N<sub>2</sub>, GHSV = 150 000 h<sup>−1</sup>.



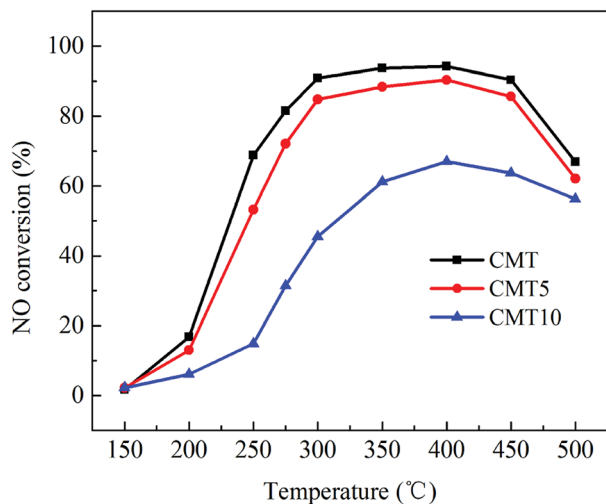


Fig. 2 Effect of H<sub>2</sub>O on NO conversion over different samples. Reaction conditions: [NO] = [NH<sub>3</sub>] = 1000 ppm, [O<sub>2</sub>] = 3%, [H<sub>2</sub>O] = 10%, balance N<sub>2</sub> and GHSV = 150 000 h<sup>-1</sup>.

250 °C to 350 °C. The N<sub>2</sub> selectivity of CMT10 decreased slightly below 250 °C and at 350–450 °C in comparison with those of CMT and CMT5. It could be seen that HCl loadings had little influence on the N<sub>2</sub> selectivity of CMT.

The effect of H<sub>2</sub>O on the SCR activities of the fresh and HCl-loaded CMT was investigated and the results are shown in Fig. 2. Compared with Fig. 1 and 2, it was found that CMT10 suffered much more serious deactivation than the other samples. The presence of H<sub>2</sub>O suppressed the NO removal process over SCR catalysts by competing with NH<sub>3</sub> adsorption on the reaction sites or occupying the oxygen vacancies in active species.<sup>6,17,18</sup> The existence of HCl on the surface of CMT was likely to aggravate the competitive adsorption of H<sub>2</sub>O with NH<sub>3</sub> and the positioning of the oxygen vacancies in Ce species.

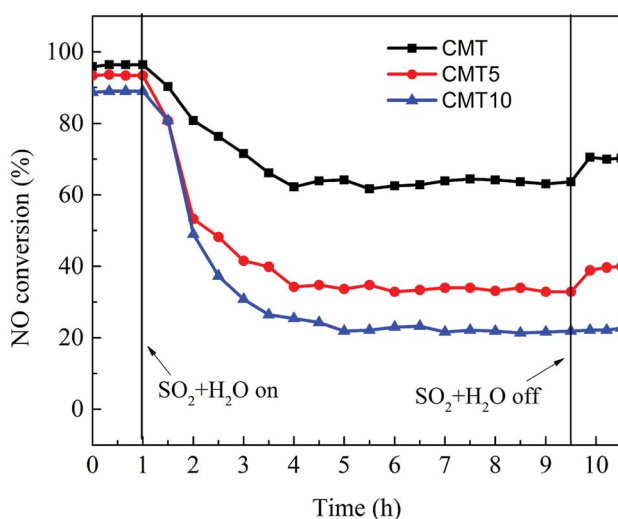


Fig. 3 Effect of H<sub>2</sub>O and SO<sub>2</sub> on NO conversion for different catalyst samples as a function of reaction temperature. Reaction conditions: [NO] = [NH<sub>3</sub>] = 1000 ppm, [O<sub>2</sub>] = 3%, [H<sub>2</sub>O] = 10%, [SO<sub>2</sub>] = 500 ppm, balance N<sub>2</sub> and GHSV = 150 000 h<sup>-1</sup>.

Fig. 3 displays the co-effect of H<sub>2</sub>O and SO<sub>2</sub> on the SCR of NO with NH<sub>3</sub> over the fresh and HCl-loaded CMT. The presence of SO<sub>2</sub> and H<sub>2</sub>O led to a rapid decrease in the SCR activities of the three samples to different extents. After about 4 hours, their activities became stable. It was clear that the resistance of CMT against SO<sub>2</sub> and H<sub>2</sub>O declined with increasing the loadings of HCl. The deactivation by SO<sub>2</sub> of Ce-based oxide SCR catalysts was believed to result from the formation of sulfate species on their surface, including NH<sub>4</sub>HSO<sub>4</sub>, Ce(SO<sub>4</sub>)<sub>2</sub> and Ce<sub>2</sub>(SO<sub>4</sub>)<sub>3</sub>.<sup>17,19,20</sup> In the presence of O<sub>2</sub>, SO<sub>2</sub> and H<sub>2</sub>O might react with NH<sub>3</sub> to produce NH<sub>4</sub>HSO<sub>4</sub>. NH<sub>4</sub>HSO<sub>4</sub> could accumulate on catalyst surface and further cover active sites.<sup>19</sup> On the other hand, SO<sub>2</sub> might combine with Ce species on catalyst surface in the presence of O<sub>2</sub> to form high thermally stable Ce(SO<sub>4</sub>)<sub>2</sub> and Ce<sub>2</sub>(SO<sub>4</sub>)<sub>3</sub>. They could hinder the Ce<sup>4+</sup>/Ce<sup>3+</sup> redox cycle and inhibit the formation and adsorption of surface nitrate species.<sup>19</sup> After SO<sub>2</sub> and H<sub>2</sub>O were cut off from the feed gas, the NO conversions over CMT and CMT5 increased slightly, while no obvious change was observed in the NO conversion over CMT10. It indicated that there might exist NH<sub>4</sub>HSO<sub>4</sub> on the surface of CMT and CMT5. After removing SO<sub>2</sub> and H<sub>2</sub>O, unstable NH<sub>4</sub>HSO<sub>4</sub> volatilized or decomposed. The deactivation of the three samples was largely caused by Ce(SO<sub>4</sub>)<sub>2</sub> and Ce<sub>2</sub>(SO<sub>4</sub>)<sub>3</sub>. The presence of HCl might promote the formation of the two sulfate species, thereby resulting in more serious deactivation of CMT10.

### 3.2. Characterization of catalysts

**3.2.1 BET and XRD analysis.** According to the BET results, it was found that the BET surface area of different samples decreased by the following order: CMT (99.06 m<sup>2</sup> g<sup>-1</sup>) > CMT5 (88.76 m<sup>2</sup> g<sup>-1</sup>) > CMT10 (81.49 m<sup>2</sup> g<sup>-1</sup>). It was clear that the BET surface area of CMT decreased with increasing Cl loadings, which was consistent with the catalytic activity (as shown in Fig. 1). Fig. 4 shows the pore size distribution of the samples. It could be seen that the pore sizes of CMT increased with increasing Cl loadings while the pore volumes fell gradually. This meant that a portion of small mesopores might be blocked

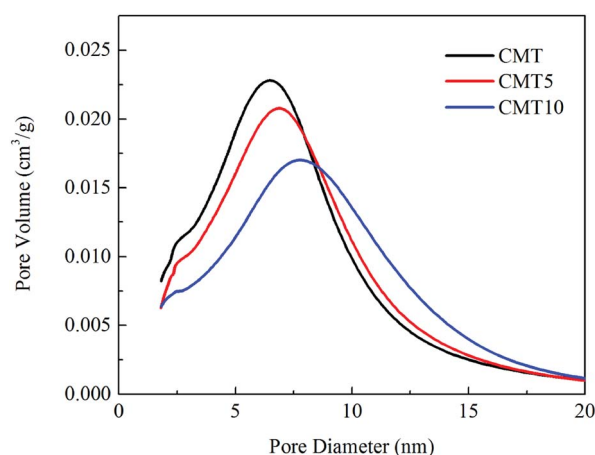


Fig. 4 Pore size distributions of the catalyst samples.

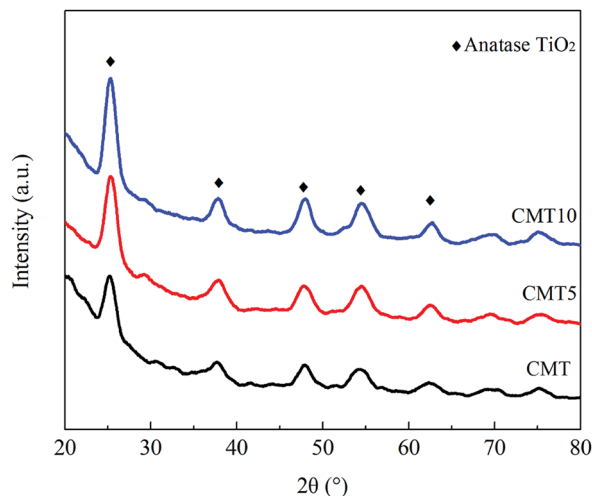


Fig. 5 XRD patterns of the catalyst samples.

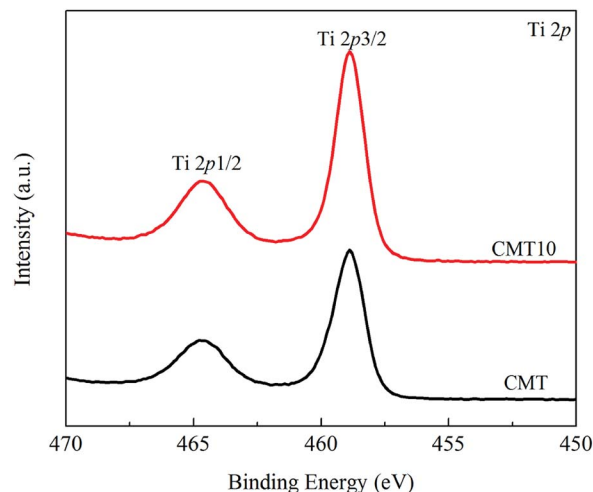


Fig. 6 XPS spectra of Ti 2p for the catalyst samples.

by chloride species. Wang *et al.*<sup>21</sup> found the similar phenomena in the study on the effect of F or Cl on Mn/TiO<sub>2</sub> catalyst.

The XRD patterns of the fresh and HCl-loaded CMT are presented in Fig. 5. Only the diffraction peaks ascribed to anatase TiO<sub>2</sub> were detected, while the characteristic peaks of CeO<sub>2</sub> and MoO<sub>3</sub> were not observed. This demonstrated that the presence of HCl had no obvious impact on the dispersion of CeO<sub>2</sub> and MoO<sub>3</sub> on the surface of TiO<sub>2</sub>. CeO<sub>2</sub> and MoO<sub>3</sub> were still highly dispersed and existed as amorphous or highly dispersed species in CMT. However, the intensity of the diffraction peaks due to anatase TiO<sub>2</sub> was found to increase with increasing Cl loadings. This meant that the presence of HCl served to weaken the interaction among CeO<sub>2</sub>, MoO<sub>3</sub> and TiO<sub>2</sub>, thereby resulting in the deactivation of CMT.

**3.2.2 XPS analysis.** The surface atomic concentrations of the catalyst samples are summarized in Table 1. The addition of HCl led to the decrease in the amount of reactive Ce and Mo atoms on the catalyst surface, which was in line with the catalytic activity. In addition, it was found that the measured Cl concentration on the catalyst surface was far lower than its nominal one. This might be due to its extraordinary high volatility.<sup>22</sup>

As shown in Fig. 6, the binding energies of Ti 2p<sub>1/2</sub> and Ti 2p<sub>3/2</sub> in different catalysts were about 464.5 and 458.5 eV, respectively.<sup>23</sup> It suggested that Ti in CMT and CMT10 existed in its highest oxidation state (IV).<sup>24</sup> There was no significant change in the peak position among the two samples, but the intensities of both peaks increased after the introduction of Cl, which was

in accordance with the XRD results. This meant that there existed an interaction between HCl and Ti.

After a curve-fitting procedure in Fig. 7, the spectra of O 1s can be deconvoluted into two peaks. The peak at about 529.7–530.1 eV could be assigned to lattice oxygen (denoted as O<sub>α</sub>) and the other one at about 531.1–531.4 eV could be related to chemisorbed oxygen (denoted as O<sub>β</sub>) from oxide defects or hydroxyl-like groups.<sup>25,26</sup> After treated by HCl, the O<sub>β</sub>/O ratio decreased from 35.21% to 23.62%, which was in good agreement with the catalytic activity. O<sub>β</sub> was considered to be more active in SCR reaction than O<sub>α</sub> because of its higher mobility.<sup>27</sup> As a result, the SCR activity of CMT decreased after loading HCl.

The deconvoluted Ce 3d XPS results of the catalyst samples are shown in Fig. 8. The peaks labeled u, u'', u''' and v, v'', v''' are assigned to Ce<sup>4+</sup>, while u' and v' are attributed to Ce<sup>3+</sup>.<sup>28,29</sup> The atomic ratio of Ce<sup>3+</sup>/Ce, calculated by the area of the corresponding peaks, increased from 31.81% to 34.76%. It indicated that the presence of HCl led to the increase in the amount of Ce<sup>3+</sup> and the decrease in the amount of Ce<sup>4+</sup> on the catalyst

**Table 1** Surface element compositions of the catalyst samples determined by XPS

Sample	Surface atomic concentration (%)						
	O	Ti	Mo	Ce	Cl	O <sub>β</sub> /O	Ce <sup>3+</sup> /Ce
CMT	66.53	27.71	3.09	2.68	—	35.21	31.81
CMT10	64.73	29.42	2.64	2.01	1.20	23.62	34.76

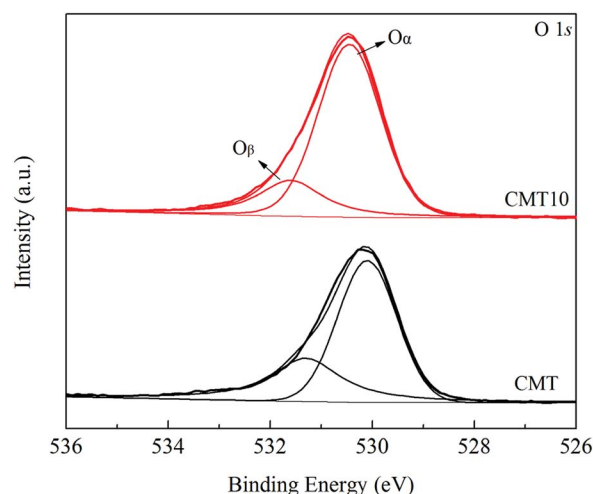


Fig. 7 XPS spectra of O 1s for the catalyst samples.





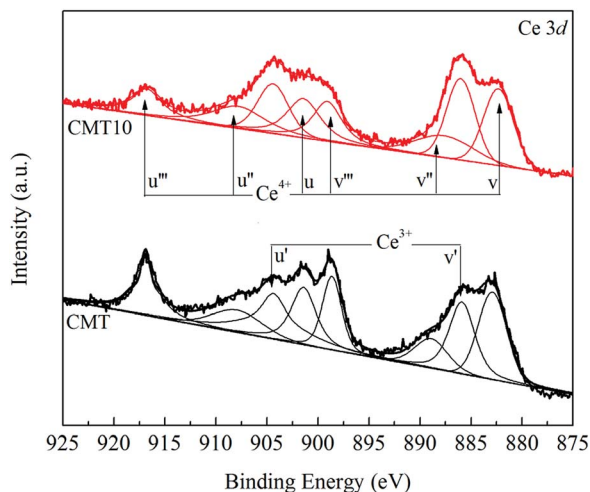


Fig. 8 XPS spectra of Ce 3d for the catalyst samples.

surface. It is widely accepted that  $\text{Ce}^{3+}$  can create a charge imbalance and form oxygen vacancies and unsaturated chemical bonds, which is helpful for the formation of chemisorbed oxygen on the catalyst surface.<sup>30</sup> However, it was unexpected that the increase in the amount of  $\text{Ce}^{3+}$  due to the presence of HCl did not promote the formation of chemisorbed oxygen. On the contrary, the amount of chemisorbed oxygen decreased. It might be supposed that not all  $\text{Ce}^{3+}$  species could act as a promoter on SCR activity.

Fig. 9 illustrates the XPS spectra of Cl 2p in CMT10. The peak appearing at 198.4 eV was assigned to  $\text{Cl}^-$ .<sup>31</sup> According to the handbook of X-ray photoelectron spectroscopy,<sup>32</sup> it could be inferred that  $\text{CeCl}_3$  molecules might form on the surface of CMT10. It could be speculated that a fraction of  $\text{CeO}_2$  might react with HCl according to the following reaction:

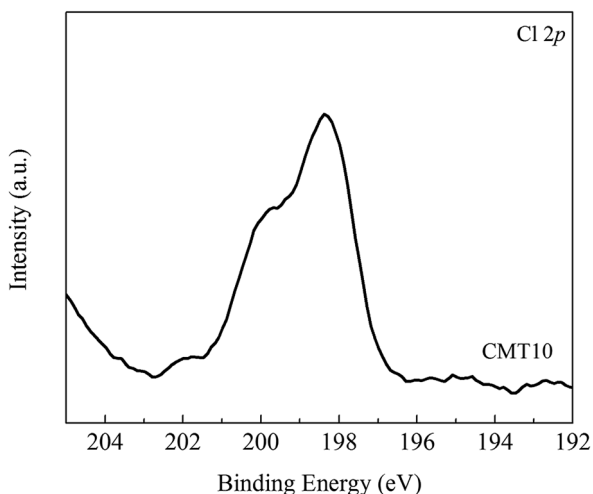
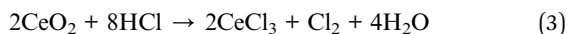


Fig. 9 XPS spectra of Cl 2p for the CMT10 sample.

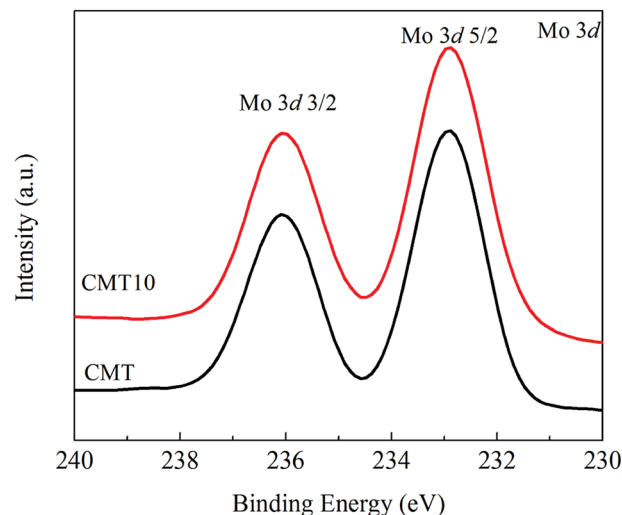


Fig. 10 XPS spectra of Mo 3d for the catalyst samples.

The presence of HCl could result in the transformation of  $\text{Ce}^{4+}$  into  $\text{Ce}^{3+}$ . However,  $\text{Ce}^{3+}$  in the form of  $\text{CeCl}_3$  lost the ability to be converted into active  $\text{Ce}^{4+}$  and was unreactive in SCR reaction. Therefore, the  $\text{Ce}^{3+}/\text{Ce}^{4+}$  redox cycle was damaged. It is generally accepted that the redox pairs of  $\text{Ce}^{3+}/\text{Ce}^{4+}$  on catalyst surface are vital for the SCR reaction over  $\text{CeO}_2$ -based catalyst.<sup>33</sup> As a result, the catalytic performance of CMT decreased.

The Mo XPS profiles of catalyst samples are shown in Fig. 10. The binding energies of  $\text{Mo } 3d_{5/2}$  and  $\text{Mo } 3d_{3/2}$  were observed at 232.6 and 235.9 eV, and both spectra of the catalysts provide typical patterns for  $\text{MoO}_3$ .<sup>34</sup> Regardless of the peak positions or intensities, there was no obvious difference between CMT and CMT10 catalyst samples. It suggested that the chemical environment of  $\text{Mo}^{6+}$  remained almost the same after the introduction of Cl. Unlike active Ce species,  $\text{MoO}_3$  supported on  $\text{TiO}_2$  was not to be highly active for the SCR reaction.<sup>17</sup>  $\text{MoO}_3$  primarily acted as a structural and chemical promoter rather than main active species. Compared with the Ce and Mo XPS results, it could be supposed that HCl preferentially reacted with active Ce species instead of Mo species. Consequently, Mo XPS curve was not changed in the presence of HCl.

**3.2.3  $\text{NH}_3$ -TPD analysis.**  $\text{NH}_3$ -TPD analysis was performed to study the surface acidity of the catalyst samples and the results are presented in Fig. 11. Each catalyst sample contained a broad  $\text{NH}_3$  desorption peak centered at about 200 °C, which could be assigned to the weakly absorbed  $\text{NH}_3$  on Brønsted acid sites.<sup>21,24</sup> As for CMT, one small peak centered at about 600 °C was observed and could be attributed to the strongly absorbed  $\text{NH}_3$  on Lewis acid sites.<sup>35</sup> The presence of HCl resulted in the decrease in the  $\text{NH}_3$  desorption peak area at low and high temperatures. Furthermore, the peak at high temperature shifted to higher temperatures. It indicated that the Brønsted acid sites and Lewis acid sites on the surface of CMT decreased, thereby inhibiting the adsorption of  $\text{NH}_3$  species on the catalyst. As a result, HCl has a negative effect on the activity of CMT.



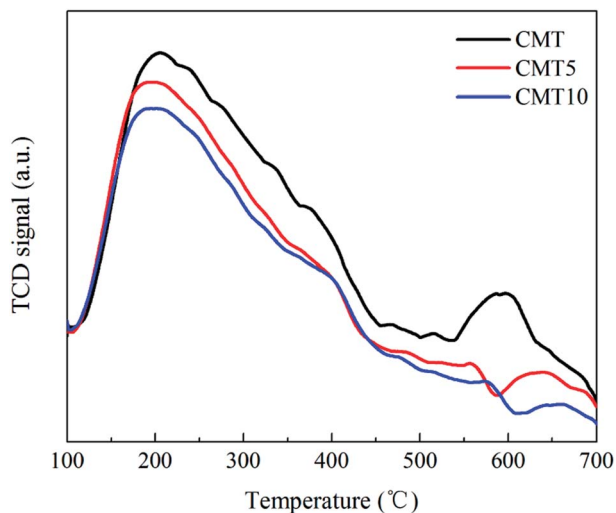


Fig. 11  $\text{NH}_3$ -TPD profiles of the catalyst samples.

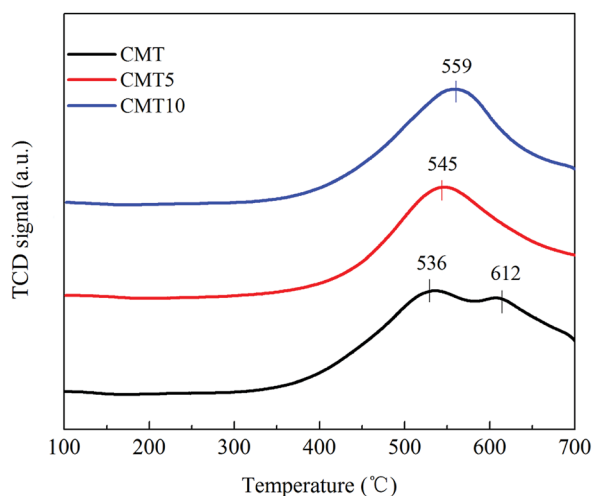


Fig. 12  $\text{H}_2$ -TPR profiles of the catalyst samples.

**3.2.4  $\text{H}_2$ -TPR analysis.** Apart from the surface acidity of the catalyst, redox property is also another key factor which influences the performance of SCR catalyst. Fig. 12 illustrated the  $\text{H}_2$ -TPR profiles of the catalyst samples. The TPR of the fresh CMT illustrated two overlapping reduction peaks, at 536 °C and 612 °C, indicating the co-reduction of surface Ce and well dispersed octahedral Mo species.<sup>36,37</sup> After adding HCl, the peak at 612 °C disappeared while the peak at 536 °C moved to higher temperature. It was possible that the introduction of HCl make the two peaks overlap. Jin *et al.*<sup>38</sup> reported the similar phenomenon on  $\text{CeO}_2/\text{TiO}_2$  catalyst with the modulation of HF. Nevertheless, the  $\text{H}_2$  consumption decreased in the order: CMT > CMT5 > CMT10. It indicated that reducibility of CMT was weakened due to the presence of HCl. It was clear that HCl should be responsible for the strong inhibition in the catalytic activity of CMT.

## 4. Conclusions

In this work, the influence of HCl on the selective catalytic reduction of NO with  $\text{NH}_3$  over  $\text{CeO}_2\text{-MoO}_3/\text{TiO}_2$  catalyst was investigated. The experimental results showed that HCl had a negative effect on the SCR performance of  $\text{CeO}_2\text{-MoO}_3/\text{TiO}_2$  catalyst. The presence of HCl led to pore blockage, weakened interaction among  $\text{CeO}_2$ ,  $\text{MoO}_3$  and  $\text{TiO}_2$ , reduction in surface acidity and degradation of redox ability. Though the amount of  $\text{Ce}^{3+}$  increased on the catalyst surface after adding HCl,  $\text{Ce}^{3+}$  in the form of  $\text{CeCl}_3$  was not active in SCR reaction. The  $\text{Ce}^{3+}/\text{Ce}^{4+}$  redox cycle was damaged. In addition, the concentration of surface Ce and Mo atoms and the amount of chemisorbed oxygen were found to decrease. All of these factors were responsible for the deactivation by HCl of CMT.

## Conflicts of interest

There are no conflicts to declare.

## Acknowledgements

This work was supported by the National Natural Science Foundation of China (No. 51506226), Natural Science Foundation of Shandong Province (No. ZR2015EM010), “the Fundamental Research Funds for the Central Universities” (No. 15CX05005A) and the scholarship from China Scholarship Council, China (CSC) (No. 201706455013).

## References

- 1 H. Chang, X. Chen, J. Li, L. Ma, C. Wang, C. Liu, W. S. Johannes and J. Hao, Improvement of activity and  $\text{SO}_2$  tolerance of Sn-modified  $\text{MnO}_x\text{-CeO}_2$  catalysts for  $\text{NH}_3$ -SCR at low temperatures, *Environ. Sci. Technol.*, 2013, 47(10), 5294–5301.
- 2 X. Du, J. Xue, X. Wang, Y. Chen, J. Ran and L. Zhang, Oxidation of sulfur dioxide over  $\text{V}_2\text{O}_5/\text{TiO}_2$  catalyst with low vanadium loading: a theoretical study, *J. Phys. Chem. C*, 2018, 122(8), 4517–4523.
- 3 L. Lietti, I. Nova and P. Forzatti, Selective catalytic reduction (SCR) of NO by  $\text{NH}_3$  over  $\text{TiO}_2$ -supported  $\text{V}_2\text{O}_5\text{-WO}_3$  and  $\text{V}_2\text{O}_5\text{-MoO}_3$  catalysts, *Top. Catal.*, 2000, 11–12, 111–122.
- 4 C. Tang, H. Zhang and L. Dong, Ceria-based catalysts for low-temperature selective catalytic reduction of NO with  $\text{NH}_3$ , *Catal. Sci. Technol.*, 2016, 6(5), 1248–1264.
- 5 R. Guo, P. Sun, W. Pan, M. Li, S. Liu, X. Sun, S. Liu and J. Liu, A highly effective  $\text{MnNdO}_x$  catalyst for the selective catalytic reduction of  $\text{NO}_x$  with  $\text{NH}_3$ , *Ind. Eng. Chem. Res.*, 2017, 56(44), 12566–12577.
- 6 X. Gao, X. Du, L. Cui, Y. Fu, Z. Luo and K. Cen, A Ce–Cu–Ti oxide catalyst for the selective catalytic reduction of NO with  $\text{NH}_3$ , *Catal. Commun.*, 2010, 12(4), 255–258.
- 7 W. Shan, F. Liu, Y. Yu and H. He, The use of ceria for the selective catalytic reduction of  $\text{NO}_x$  with  $\text{NH}_3$ , *Chin. J. Catal.*, 2014, 35, 1251–1259.



- 8 Z. Liu, H. Su, J. Li and Y. Li, Novel  $\text{MoO}_3/\text{CeO}_2\text{-ZrO}_2$  catalyst for the selective catalytic reduction of  $\text{NO}_x$  by  $\text{NH}_3$ , *Catal. Commun.*, 2015, **65**, 51–54.
- 9 Z. Liu, Y. Yi, J. Li, S. Woo, B. Wang, X. Cao and Z. Li, A superior catalyst with dual redox cycles for the selective reduction of  $\text{NO}_x$  by ammonia, *Chem. Commun.*, 2013, **49**(70), 7726–7728.
- 10 Z. Liu, J. Zhu, J. Li, L. Ma and S. Woo, Novel Mn–Ce–Ti mixed-oxide catalyst for the selective catalytic reduction of  $\text{NO}_x$  with  $\text{NH}_3$ , *ACS Appl. Mater. Interfaces*, 2014, **6**, 14500–14508.
- 11 Y. Jiang, Z. Xing, X. Wang, S. Huang, Q. Liu and J. Yang,  $\text{MoO}_3$  modified  $\text{CeO}_2/\text{TiO}_2$  catalyst prepared by a single step sol–gel method for selective catalytic reduction of NO with  $\text{NH}_3$ , *J. Ind. Eng. Chem.*, 2015, **29**, 43–47.
- 12 J. P. Chen, M. A. Buzanowski, R. T. Yang and J. E. Cichanowicz, Deactivation of the vanadia catalyst in the selective catalytic reduction process, *J. Air Waste Manage. Assoc.*, 1990, **40**(10), 1403–1409.
- 13 L. Lisi, G. Lasorella, S. Malloggi and G. Russo, Single and combined deactivating effect of alkali metals and HCl on commercial SCR catalysts, *Appl. Catal., B*, 2004, **50**(4), 251–258.
- 14 N. Z. Yang, R. T. Guo, W. G. Pan, *et al.* The deactivation mechanism of Cl on  $\text{Ce}/\text{TiO}_2$  catalyst for selective catalytic reduction of NO with  $\text{NH}_3$ , *Appl. Surf. Sci.*, 2016, **378**, 513–518.
- 15 Y. Hou, G. Cai, Z. Huang, X. Han and S. Guo, Effect of HCl on  $\text{V}_2\text{O}_5/\text{AC}$  catalyst for NO reduction by  $\text{NH}_3$  at low temperatures, *Chem. Eng. J.*, 2014, **247**, 59–65.
- 16 X. Yu, F. Cao, X. Zhu, X. Zhu, X. Gao, Z. Luo and K. Cen, Selective catalytic reduction of NO over Cu–Mn/OMC catalysts: effect of preparation method, *Aerosol Air Qual. Res.*, 2017, **17**, 302–313.
- 17 Y. Jiang, X. Zhang, M. Lu, C. Bao, G. Liang, C. Lai, W. Shi and S. Ma, Activity and characterization of Ce–Mo–Ti mixed oxide catalysts prepared by a homogeneous precipitation method for selective catalytic reduction of NO with  $\text{NH}_3$ , *J. Taiwan Inst. Chem. Eng.*, 2018, **86**, 133–140.
- 18 M. Casapu, O. Kröcher and M. Elsener, Screening of doped  $\text{MnO}_x\text{-CeO}_2$  catalysts for low-temperature NO-SCR, *Appl. Catal., B*, 2009, **88**, 413–419.
- 19 W. Xu, H. He and Y. Yu, Deactivation of a  $\text{Ce}/\text{TiO}_2$  catalyst by  $\text{SO}_2$  in the selective catalytic reduction of NO by  $\text{NH}_3$ , *J. Phys. Chem.*, 2009, **113**, 4426–4432.
- 20 Y. Peng, C. Liu, X. Zhang and J. Li, The effect of  $\text{SiO}_2$  on a novel  $\text{CeO}_2\text{-WO}_3/\text{TiO}_2$  catalyst for the selective catalytic reduction of NO with  $\text{NH}_3$ , *Appl. Catal., B*, 2013, **140–141**, 276–282.
- 21 P. Wang, Q. S. Wang, X. X. Ma, R. T. Guo and W. G. Pan, The influence of F and Cl on Mn/ $\text{TiO}_2$ , catalyst for selective catalytic reduction of NO with  $\text{NH}_3$ : a comparative study, *Catal. Commun.*, 2015, **71**, 84–87.
- 22 X. Wu, W. Yu, Z. Si and D. Weng, Chemical deactivation of  $\text{V}_2\text{O}_5\text{-WO}_3/\text{TiO}_2$  SCR catalyst by combined effect of potassium and chloride, *Front. Environ. Sci. Eng.*, 2013, **7**(3), 420–427.
- 23 X. Gao, Y. Jiang, Y. Zhong, Z. Luo and K. Cen, The activity and characterization of  $\text{CeO}_2\text{-TiO}_2$  catalysts prepared by the sol–gel method for selective catalytic reduction of NO with  $\text{NH}_3$ , *J. Hazard. Mater.*, 2010, **174**(1–3), 734–739.
- 24 X. Du, X. Gao, L. Cui, Y. Fu, Z. Luo and K. Cen, Investigation of the effect of Cu addition on the  $\text{SO}_2$ -resistance of a CeTi oxide catalyst for selective catalytic reduction of NO with  $\text{NH}_3$ , *Fuel*, 2012, **92**(1), 49–55.
- 25 Y. Peng, K. Li and J. Li, Identification of the active sites on  $\text{CeO}_2\text{-WO}_3$  catalysts for SCR of  $\text{NO}_x$  with  $\text{NH}_3$ : an *in situ* IR and Raman spectroscopy study, *Appl. Catal., B*, 2013, **140–141**, 483–492.
- 26 N. Z. Yang, R. T. Guo, W. G. Pan, Q. L. Chen, Q. S. Wang and C. Z. Lu, The promotion effect of Sb on the Na resistance of Mn/ $\text{TiO}_2$  catalyst for selective catalytic reduction of NO with  $\text{NH}_3$ , *Fuel*, 2016, **169**, 87–92.
- 27 H. Chang, J. Li, J. Yuan, L. Chen, Y. Dai, A. Hamidreza, J. Xu and J. Hao, Ge, Mn-doped  $\text{CeO}_2\text{-WO}_3$  catalysts for  $\text{NH}_3\text{-SCR}$  of  $\text{NO}_x$ : effects of  $\text{SO}_2$  and  $\text{H}_2$  regeneration, *Catal. Today*, 2013, **201**(1), 139–144.
- 28 W. Shan, F. Liu, H. He, X. Shi and C. Zhang, A superior Ce–W–Ti mixed oxide catalyst for the selective catalytic reduction of  $\text{NO}_x$  with  $\text{NH}_3$ , *Appl. Catal., B*, 2012, **115–116**, 100–106.
- 29 D. Devaiah, D. Jampaiah, P. Saikia and B. M. Reddy, Structure dependent catalytic activity of  $\text{Ce}_{0.8}\text{Tb}_{0.2}\text{O}_{2-\delta}$  and  $\text{TiO}_2$  supported  $\text{Ce}_{0.8}\text{Tb}_{0.2}\text{O}_{2-\delta}$  solid solutions for CO oxidation, *J. Ind. Eng. Chem.*, 2014, **20**(2), 444–453.
- 30 R. T. Guo, C. Z. Lu, W. G. Pan, W. L. Zhen, Q. S. Wang, Q. L. Chen, H. L. Ding and N. Z. Yang, A comparative study of the poisoning effect of Zn and Pb on  $\text{Ce}/\text{TiO}_2$  catalyst for low temperature selective catalytic reduction of NO with  $\text{NH}_3$ , *Catal. Commun.*, 2015, **59**, 136–139.
- 31 F. Y. Chang, J. C. Chen and M. Y. Wey, Activity and characterization of  $\text{Rh}/\text{Al}_2\text{O}_3$  and  $\text{Rh-Na}/\text{Al}_2\text{O}_3$  catalysts for the SCR of NO with CO in the presence of  $\text{SO}_2$  and HCl, *Fuel*, 2010, **89**(8), 1919–1927.
- 32 C. Wagner, W. Riggs, L. Davis, J. Moulder and G. Muilenberg, *Hand book of X-Ray Photoelectron Spectroscopy*, Perkin-Elmer Corporation, 1st. minnesota, 1979.
- 33 X. Li, X. Li, J. Li and L. Hao, Identification of the arsenic resistance on  $\text{MoO}_3$  doped  $\text{CeO}_2/\text{TiO}_2$  catalyst for selective catalytic reduction of  $\text{NO}_x$  with ammonia, *J. Hazard. Mater.*, 2016, **318**, 615–622.
- 34 H. L. Koh and H. K. Park, Characterization of  $\text{MoO}_3\text{-V}_2\text{O}_5/\text{Al}_2\text{O}_3$  catalysts for selective catalytic reduction of NO by  $\text{NH}_3$ , *J. Ind. Eng. Chem.*, 2013, **19**(1), 73–79.
- 35 R. Zhang, Q. Zhong, W. Zhao, *et al.* Promotional effect of fluorine on the selective catalytic reduction of NO with  $\text{NH}_3$  over  $\text{CeO}_2\text{-TiO}_2$  catalyst at low temperature, *Appl. Surf. Sci.*, 2014, **289**(289), 237–244.
- 36 Z. Liu, S. Zhang, J. Li and L. Ma, Promoting effect of  $\text{MoO}_3$  on the  $\text{NO}_x$  reduction by  $\text{NH}_3$  over  $\text{CeO}_2/\text{TiO}_2$  catalyst studied with *in situ* DRIFTS, *Appl. Catal., B*, 2014, **144**(1), 90–95.



- 37 L. Caero, A. Romero and J. Ramirez, Niobium sulfide as a dopant for Mo/TiO<sub>2</sub> catalysts, *Catal. Today*, 2003, **78**, 513–518.
- 38 Q. Jin, Y. Shen and S. Zhu, Effect of fluorine additive on CeO<sub>2</sub>(ZrO<sub>2</sub>)/TiO<sub>2</sub> for selective catalytic reduction of NO by NH<sub>3</sub>, *J. Colloid Interface Sci.*, 2017, **487**, 401–409.

